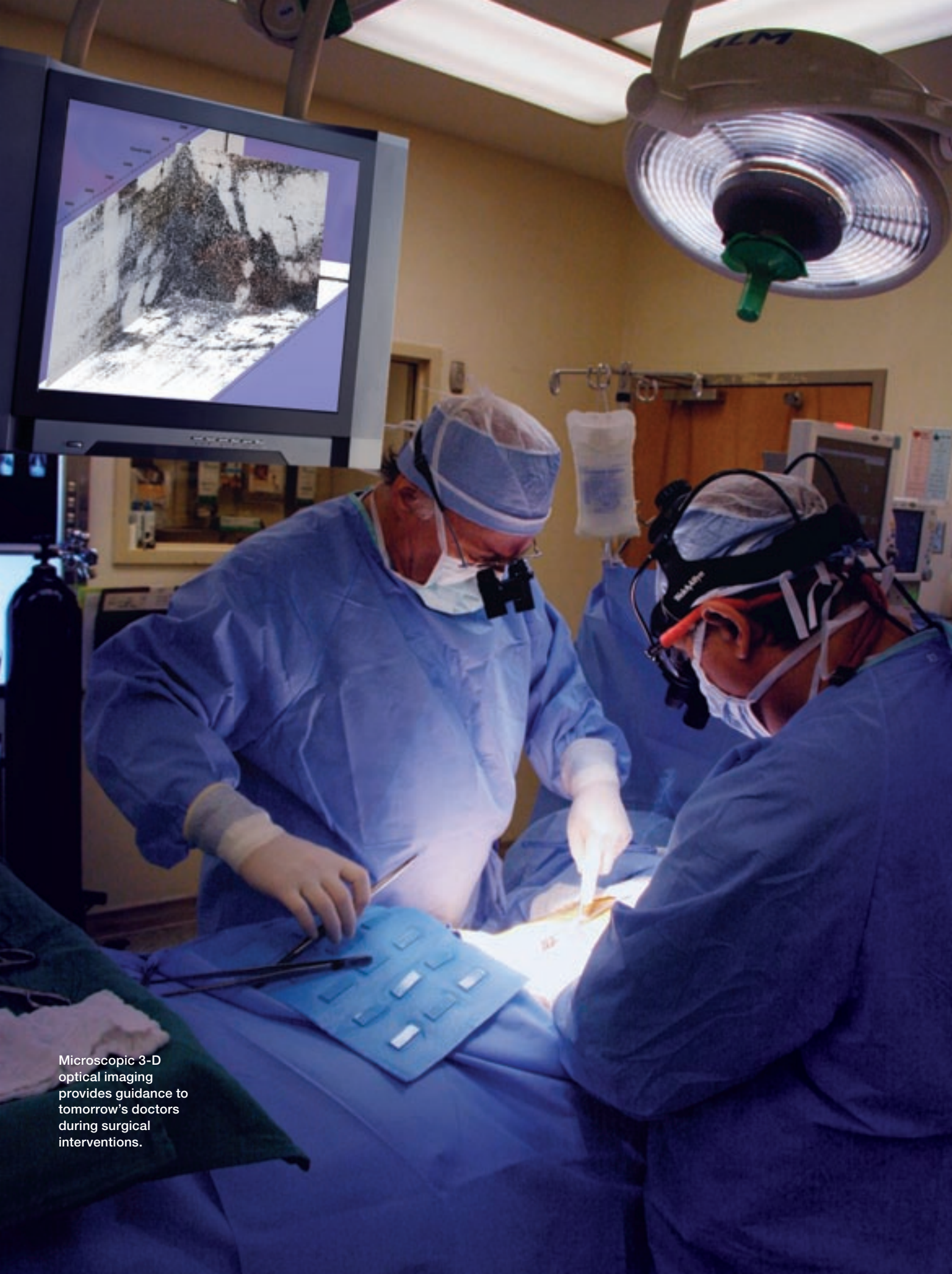

Microscopic 3-D optical imaging provides guidance to tomorrow's doctors during surgical interventions.

LASERFEST

Interferometric Synthetic Aperture Microscopy

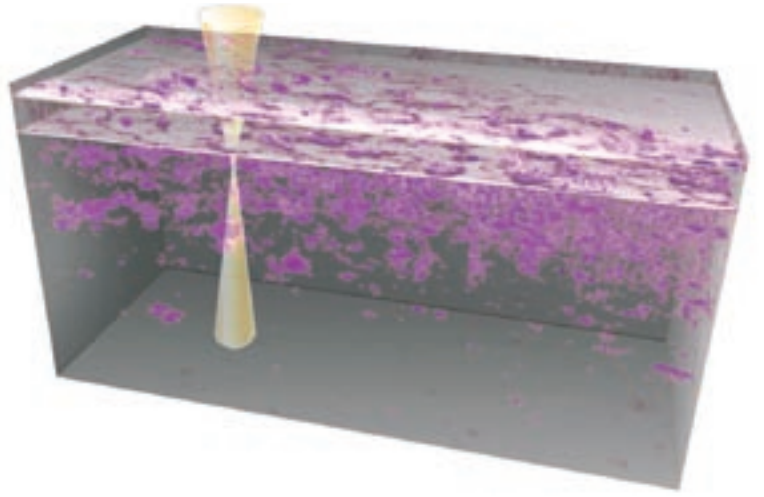

Microscopic Laser Radar

Tyler S. Ralston, Gregory L. Charvat, Steven G. Adie, Brynmor J. Davis, P. Scott Carney and Stephen A. Boppart

Combining optical coherence tomography instrumentation and the principles of synthetic aperture radar, researchers have developed a new method for reconstructing 3-D optical images—even in regions that are out of focus in the raw data. Doctors may soon be able to use this approach as a noninvasive diagnostic tool in clinical settings.

Composite image by Fran Harrington

1047-6938/10/06/0032/6-$15.00 ©OSA

In many clinical scenarios, doctors require high-resolution visualization of tissues and their underlying cellular structures. Perhaps the most common example is for the identification, diagnosis and treatment of cancer. In such cases, clinicians typically take tissue biopsies, which are then processed in a pathology lab and examined under a microscope.

A drawback of histological tissue processing is that it can take anywhere from a few hours to several days to complete. In critical operating room procedures, more timely feedback would be highly desirable. Furthermore, biopsies are often inconvenient and uncomfortable for patients, and they introduce possibilities for error into the sampling technique, since tissues are altered and disturbed as they are taken.

The ideal diagnostic modality would be noninvasive and would produce quick, accurate information in clinical settings. A new approach called interferometric synthetic aperture microscopy (ISAM) provides a means of retrieving high-resolution images from entire tissue volumes. The hardware used in ISAM originates from optical coherence tomography (OCT), a low-coherence interferometric ranging technique with micrometer-resolution and deep penetration within tissues (on the order of 2 mm). ISAM data processing is an optical analogue of synthetic aperture radar (SAR).

New advances in algorithms and computing hardware have enabled real-time ISAM—an important step toward widespread clinical use.

ISAM explicitly accounts for the optical system being used—for example, the optical beam profile, scanning pattern, bandwidth, etc. It takes advantage of the fact that the data are samples of a linear function of the scattered optical fields, and that the fields are connected to the object susceptibility function through Maxwell's equations. The susceptibility function, or a filtered version of it, is determined from data by solving this system of equations. ISAM achieves spatially invariant resolution, thus yielding advantages over OCT, which has comparable resolution only in the focal plane. Spatially invariant resolution extends the functionality of the imaging system by distinguishing structural scattering from beam-defocusing effects. New advances in algorithms and computing hardware have enabled real-time ISAM—an important step toward widespread clinical use.

[Spectral-domain OCT system and ISAM algorithm]

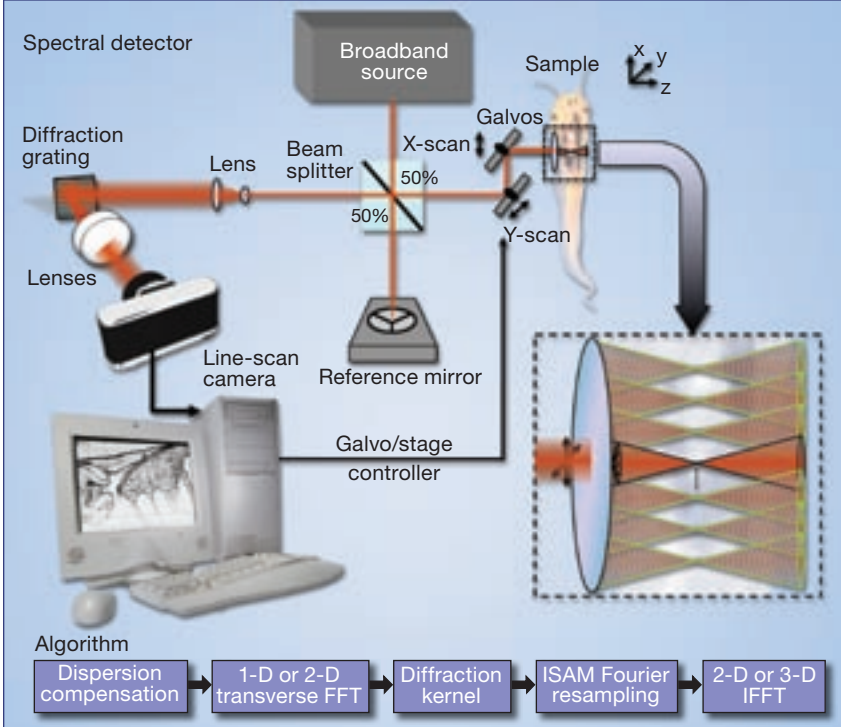

(Top) A spectral domain optical coherence tomography (SD-OCT) system used for phase stable ISAM measurements. A broadband source feeds into a beam splitter, where 50 percent serves as a reference for the other 50 percent traveling to and scattered back from the sample. Scattering depths are inferred from the spectral interference. The beam is scanned over an objective lens that focuses it into the specimen. (Bottom) To form images, the data are processed with the ISAM algorithm on a personal computer.

Optical coherence tomography

The figure to the left illustrates an implementation of OCT, known as spectral-domain OCT (SD-OCT). OCT is a high-resolution medical and biological imaging technology that is making the transition from research technique into clinical tool. It is analogous to imaging techniques such as radar, sonar or medical ultrasound in as much as it relies on "echo" time-of-flight measurements to probe an object of interest.

OCT is attractive for medical imaging because it permits real-time *in situ* imaging of tissue microstructure with a resolution (1-10 μm) that approaches that of conventional histology. Yet, in principle, there is no need to excise tissue or perform time-consuming histological processing. The technology is flexible enough to be widely applied in clinical settings because it is compatible with fixed or handheld probes, forward imaging endoscopes, fiber-optic catheters and needle-based probes.

OCT has already found widespread application in ophthalmology, due largely to the relative transparency of ocular tissues. The superior resolving capabilities of OCT over

confocal scanning laser ophthalmoscopes have made it the modality of choice for the clinical imaging of many retinal diseases. Fiber-optic catheter technology has enabled the application of OCT in cardiology, specifically for the detection of vulnerable plaques.

For all its successes, OCT has been plagued by a trade-off between resolution and depth-of-field. ISAM provides a means to circumvent this by reconstructing the underlying 3-D sample structure with spatially uniform resolution, even in those regions that appear out-of-focus in OCT. That is, the ISAM reconstruction offers depth-of-field limited only by signal power decay or by other corruption of the signal such as multiple scattering.

ISAM and OCT are derived from low-coherence interferometry, a method for measuring the travel time of backscattered light.

Synthetic aperture radar

Synthetic aperture radar is built on the instrumentation developed for radar. It provides images that are more immediately accessible and useful than the raw data from radar. While ISAM was developed from the solution of the inverse-scattering problem of OCT, the algorithm is similar to that used in SAR. This might be expected, since both systems measure fields governed by Maxwell's equations. Even though the wavelengths differ by five to six orders of magnitude, the other size scales, such as feature and detector size, scale similarly, and Maxwell's equations remain unchanged under an overall scaling of coordinates. Radar and optical ranging differ in that a deterministic phase is measured using a local oscillator (or reference chirp) in SAR, while in ISAM the phase must be captured in a statistical setting using interferometry.

The success of OCT is much like the early success of radar. High demand for images motivated advanced instrument development. Commercial OCT systems provide three-dimensional microscopic imaging in medical applications, notably in ophthalmology. Early high-resolution radar provided aircraft crews with real-time ground mapping. In each modality, the study of the physics has led to more sophisticated means to collect and interpret data.

The figure to the right illustrates an implementation of ground-based stripmap radar, known as rail SAR. Its implementation closely parallels the Cartesian scanning geometry of ISAM.

ISAM instrumentation

ISAM and OCT are derived from low-coherence interferometry (LCI), a method for measuring the travel time of backscattered light. The phase of electromagnetic fields at optical frequencies fluctuates too quickly to be measured directly, unlike microwave frequencies, for example. An interferometer can be seen as a statistical measuring device for determining the optical delay through cross-correlation.

Light from a broadband source is split into two arms, and the resulting interference between the sample and reference arms is measured at a detector. SD-OCT uses a spectral detector that measures the time-averaged intensity of the power spectral density. The backscattering delays are then calculated via the Wiener-Khintchine theorem—i.e., by Fourier transform processing. Galvanometer mirrors and translational stages in the sample arm scan a focused beam laterally across the sample to generate two- or three-dimensional datasets.

[Rail SAR system and RMA algorithm]

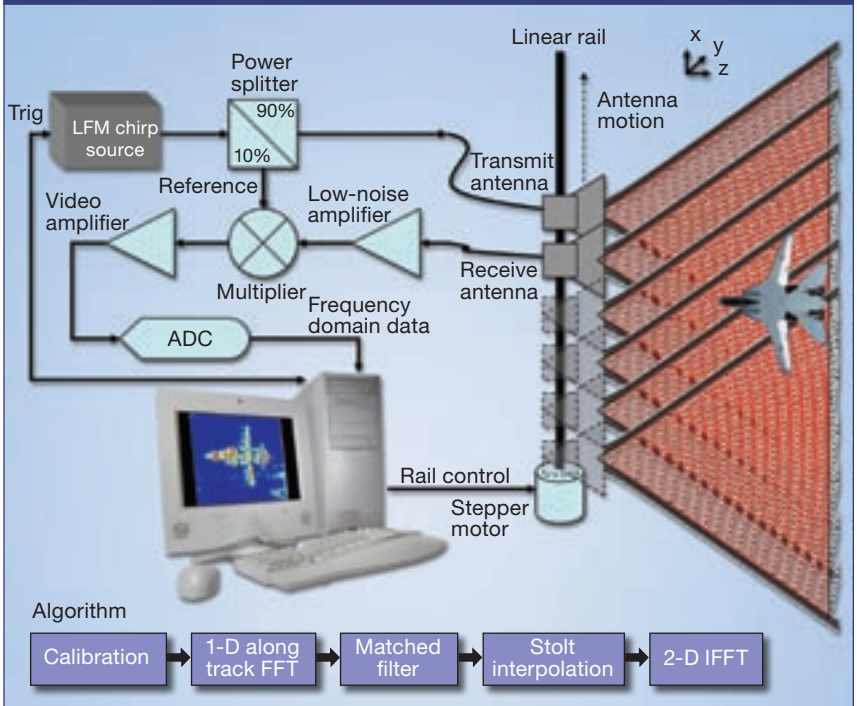

(Top) A small short-range ultrawideband radar sensor acquires range profiles for each increment along a linear path. A noticeable difference between the ISAM and SAR systems is that the ISAM system probes with a focused beam, while the SAR system probes with a divergent beam. The focal plane in the SAR system is at the front of the antenna. Transmit and receive antennas have a beamwidth of 25 degrees and the down-range target remains illuminated for the whole scan. Similar to ISAM, adjacent beams in SAR have a large overlap. (Bottom) Range profiles are processed using the range migration algorithm (RMA) to form a high-resolution image. The steps of the RMA closely parallel the inverse-scattering procedure for ISAM.

The scanning geometry dictates the structure of the reconstruction algorithm. As with OCT, several geometries can be used in ISAM, as long as the reconstruction algorithm is applied correctly. In this article, we focus on ISAM reconstruction for the commonly used Cartesian lateral beam scanning geometry, i.e., beam scanning transverse to the lens axis.

Axial resolution is inversely proportional to the bandwidth of the light source, and lateral resolution is inversely proportional to the numerical aperture (NA) of the focusing optics. In OCT, there is a trade-off between the axial range that is in focus and the achievable lateral resolution. In ISAM, this trade-off is eliminated, and spatially invariant lateral resolution is obtained at all depths in a single volumetric reconstruction.

ISAM reconstruction

The steps of the ISAM reconstruction algorithm may be applied in 2-D or 3-D. For completeness, the signal will be represented in 3-D coordinates. The SD-OCT signal may be represented by $S(x, y, \omega)$, a function of transverse position x and y, and frequency ω collected at the spectrometer. Prior to processing, the complex analytic signal representing the range profile is calculated with the digital Hilbert transform. Preprocessing steps may be applied to mitigate phase and position instabilities.

Calibration and transverse frequency

One can calibrate the SD-OCT system with a method known as dispersion correction, which is used to compensate for a mismatch of material dispersion between the sample and reference arms, or non-linear frequency dispersion introduced by the diffraction grating in the spectral detector. Digital dispersion compensation is the approach used for mapping the data from temporal frequency ω to spatial frequency k, the wavenumber.

A mirror acts as a single reflector and is used to calibrate the axial point spread function. A cubic polynomial provides a parameterized mapping formula for the conversion to spatial frequency $k(\omega)$. After mapping ω to k, the data may be rewritten as $S(x, y, k)$. The reconstruction up to this point is similar to standard processing for OCT.

In the spatial domain, each data point is the sum of contributions from all scatterers in the object—that is, the measurements are multiplexed. However, the kernel of the operator relating the object structure and the data is diagonal in transverse Fourier basis. In order to take advantage of this, one must apply the Fourier transform in the transverse directions. The signal is then written in the Fourier space of the data $S(q_x, q_y, k)$, where q_x and q_y are the transverse spatial frequency coordinates.

Move scene center, Fourier remapping and inverse Fourier transform

An important step in the inverse scattering procedure is to shift the coordinate origin to the optical focus. This can be done by shifting the phase of the data by:

$$\Phi(q_x, q_y, k) = -z_0(2k) + z_0\sqrt{(2k)^2 - q_x^2 - q_y^2}\ ,$$

where z_0 is the distance to the coordinate origin. The first term $-z_0(2k)$ shifts the data down, while the second term $z_0\sqrt{(2k)^2 - q_x^2 - q_y^2}$, a diffraction kernel, shifts and diffracts the data up. Therefore, the net movement of the sample is zero, but the net movement of the focus is z_0.

[ISAM of titanium dioxide particles suspended in a silicone matrix]

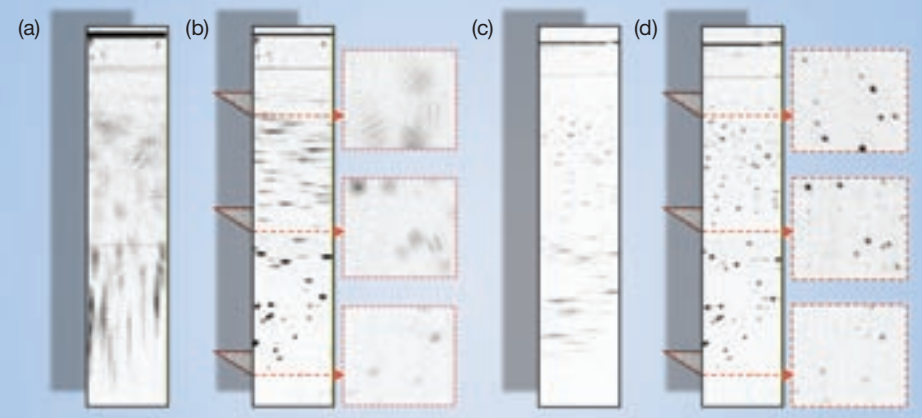

A tissue phantom consisting of subresolution-sized titanium-dioxide particles suspended in silicone is imagined with the SD-OCT system. A cross-sectional image, 100 µm (transverse) × 1.7 mm (axial), is shown (a) without any calibration (b) with system dispersion calibration (OCT) (c) with diffraction kernel adjustment and (d) with ISAM processing. *En face* planes, 100 × 120 µm, are shown to the right of (b) and (d) at three depth locations 1,100 µm above the focus, 475 µm above the focus, and 240 µm below the focus.

[Stolt resampling grid]

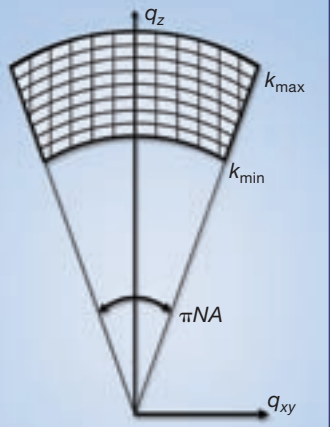

Stolt interpolation grid showing the sampling lattice for selected (q_{xy}, k) values on a uniform (q_{xy}, q_z) grid. The numerical aperture (NA) dictates the area subtended by πNA.

The Stolt interpolation is the application of a Fourier space mapping from $S(q_x, q_y, k)$ to $S(q_x, q_y, q_z)$, where the longitudinal spatial frequency coordinate is:

$$q_z = -\sqrt{(2k)^2 - q_x^2 - q_y^2}\,.$$

In the Fourier re-mapping, $q_{xy} = \sqrt{q_x^2 + q_y^2}$ is the transverse vector magnitude, k_{min} is the minimum wavenumber, and k_{max} is the maximum wavenumber.

The inverse Fourier transform is applied to $S(q_x, q_y, q_z)$ to recover the scattering potential $\eta(x, y, z)$. Aperture weights may be applied prior to this step to control the impulse response sidelobes. A multiplicative term may be applied to ISAM data to compensate for signal loss away from the focus.

The inverse-scattering solution provides a reconstruction procedure based on the model of the instrument.

ISAM experimental results

The inverse-scattering solution provides a reconstruction procedure based on the model of the instrument. However, experimental validation is required to test model assumptions and demonstrate the utility of the method. Here, we describe an experiment to test the applicability of ISAM to human tumor tissue imaging.

The ISAM system in these experiments has a near-infrared titanium-sapphire laser source with 100 nm of bandwidth centered at 800 nm. The power incident on the sample was 8 mW. The focal length of the imaging lens is 12 mm; the spot radius is 5.6 μm and the numerical aperture is 0.05. The spectrometer was designed with a 100-mm focal length achromatic lens to expand the beam before dispersion off a diffraction grating.

We used a pair of achromatic lenses to focus the dispersed optical spectrum onto a line-scan camera. The specimen was placed on the stage, and 3-D image data were measured by raster-scanning the incident beam in the transverse plane using a pair of galvanometer scanning mirrors and/or the stage.

We used the ISAM system to perform three-dimensional *ex vivo* imaging of human tumors. The ISAM reconstructions exhibit various distinguishing characteristics that are not

[ISAM of human breast adipose and tumor tissue]

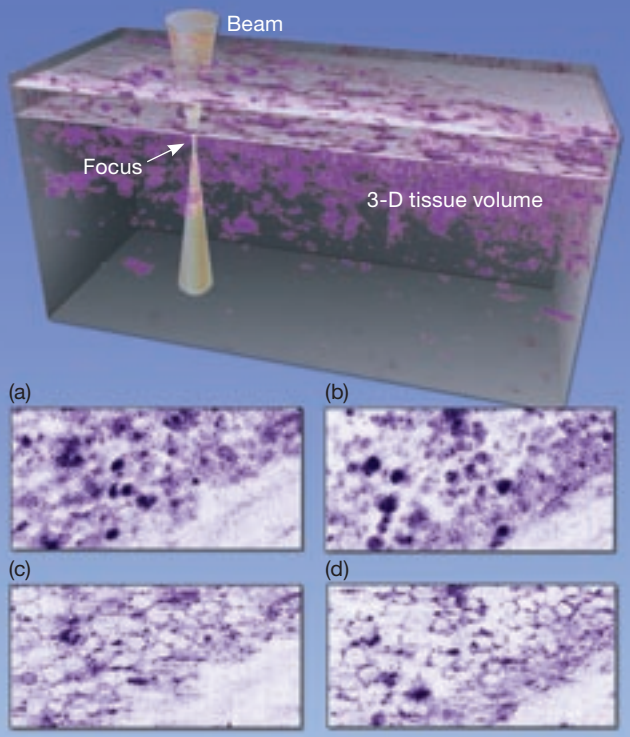

En face images from human breast tissue are shown for depths located at (a, c) z = 601 μm and (b, d) z = 653 μm where z = 0 μm is the focal plane. The unprocessed OCT data are seen on the top and the ISAM reconstructions on the bottom. The ISAM reconstructions resolve features in the tissue, which are not discernable from the unprocessed data.

[3-D ISAM of human neck tumor]

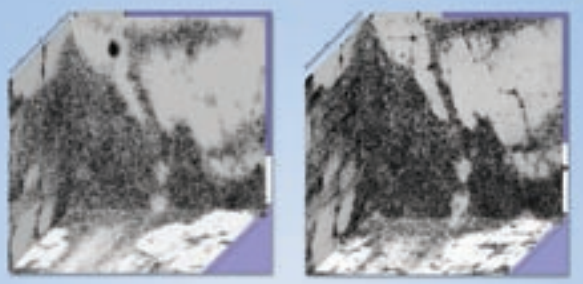

A volume of densely scattered excised human neck tumor, 360 μm × 360 μm (transverse) × 2,000 μm (axial), was imaged *ex vivo*. A sliced subset volume of (left) 3-D OCT data and (right) 3-D ISAM reconstruction are displayed. The 3-D ISAM reconstruction sharply resolves the tumor boundaries and features of the tissue. The *en face* plane is over 10 Rayleigh ranges above the focus.

[*En face* ISAM of human breast tumor tissue]

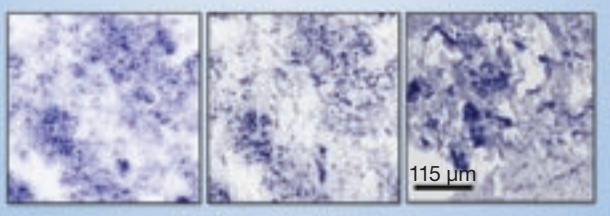

A volume of excised human tumor tissue, 360 μm × 360 μm (transverse) × 2,000 μm (axial), was imaged *ex vivo*. The *en face* data eight Rayleigh ranges from the focus is shown for (left) the OCT data, (center) the 3-D ISAM reconstruction, and (right) the corresponding histological slice.

apparent in the corresponding OCT. These include sharp boundaries of dense scattering neck tumor and adipose cells with point scatterers (cell nuclei) in breast tissue. A disruption of normal breast tissue structure accompanied by a heterogeneous clustering of cell nuclei can be observed in ISAM and histology. Note that histological processing physically alters the tissue, and thus the sample structure may be altered considerably before microscopic examination. In addition, sampling errors resulting from coarsely spaced tissue sections can increase the odds of a false-negative diagnosis. With ISAM, a clinician can inspect images of the tissue directly, rather than waiting for standard histopathology.

The visualization and analysis of 3-D volumetric data could allow for large volumes of living tissue to be imaged at cellular resolution without resection.

Ongoing research

Further research seeks to obtain cellular resolution in scattering tissues. Neoplastic changes—or changes that indicate abnormal cell growth—are characterized by abnormalities in the cellular nuclei, an accelerated rate of growth, and invasion of the cells into nearby tissues. The need to image tissue structure at the micron scale motivates the development of new ultrabroadband optical sources for micron-scale axial resolutions. However, lateral resolutions are often an order-of-magnitude higher (poorer) so as to achieve a large depth-of-field. The incorporation of ISAM thus has the potential to significantly increase diagnostic information by providing isotropic ultrahigh resolution without loss of depth-of-field. The visualization and analysis of 3-D volumetric data could allow for large volumes of living tissue to be imaged at cellular resolution without resection.

ISAM has been implemented on a portable OCT system, enabling an intraoperative feasibility study to assess the margins of resected breast tumors. Research into the development of high-NA ISAM continues, as does its application to imaging neoplastic changes.

Beyond the implementation of a planar-scanning ISAM system, researchers are studying and developing alternative instrument-scanning geometries. Rotationally scanned ISAM is compatible with catheter-based imaging, where the aperture is scanned in one linear dimension (along the catheter) and one rotational dimension (along the azimuthal angle). In full-field ISAM, a spatially extended coherent wave illuminates the sample and the scattered light is imaged onto a 2-D detector array.

ISAM signal processing algorithm development continues with research to increase processing speed and improve methods to maintain phase stability, account for nonlinear scanning, minimize axial and transverse sidelobes, and account for heterogeneities in the background sample index of refraction. Valuable insights into many of these problems may be gained from the SAR literature.

Summary

ISAM provides spatially invariant resolution, extending the depth-of-field and reducing defocusing artifacts in clinical 3-D imaging. Volumetric data with spatially invariant resolution has the potential to improve system effectiveness for the many applications of OCT imaging.

ISAM and SAR reconstruction algorithms are based on the same principle, namely that an aperture with high resolution can be computed from several low-resolution apertures. Further development of ISAM may benefit from the long history of SAR, in both reconstruction and hardware. The use of well-developed SAR algorithms such as ground moving target indication, autofocus, automatic target identification, and others can be applied to future ISAM imaging systems, providing automatic detection algorithms or guidance for diagnosis and intervention.

Tyler S. Ralston (tralston@ll.mit.edu) and Gregory L. Charvat are with the Massachusetts Institute of Technology's Lincoln Laboratory, Lexington, Mass., U.S.A. Brynmor J. Davis is with Creare, Inc., Hanover, N.H., U.S.A. **P. Scott Carney**, **Stephen A. Boppart** and Steven G. Adie are with the ECE department at the University of Illinois at Urbana-Champaign, Ill., U.S.A.

[References and Resources]

- >> G.J. Tearney et al. "Determination of the Refractive-Index of Highly Scattering Human Tissue by Optical Coherence Tomography," Opt. Lett. **20**(21), 2258-60 (1995).
- >> W.G. Carrara et al. *Spotlight Synthetic Aperture Radar Signal Processing Algorithms*, Artech House Inc., Norwood, Mass., 1995.
- >> J.M. Schmitt. "OCT elastography: imaging microscopic deformation and strain of tissue," Opt. Express **3**(6), 199-211 (1998).
- >> C. Pitris et al. "Feasibility of optical coherence tomography for high-resolution imaging of human gastrointestinal tract malignancies," J. Gastroenterol. **35**(2), 87-92 (2000).
- >> J.F. de Boer and T.E. Milner. "Review of polarization sensitive optical coherence tomography and Stokes vector determination," J. Biomed. Opt. **7**(3), 359-71 (2002).
- >> J.G. Fujimoto. "Optical coherence tomography for ultrahigh resolution *in vivo* imaging," Nature Biotech. **21**(11), 1361-7 (2003).
- >> B.E. Bouma et al. "Evaluation of intracoronary stenting by intravascular optical coherence tomography," Heart **89**(3), 317-20 (2003).
- >> D.L. Marks et al. "Inverse scattering for rotationally scanned optical coherence tomography," J. Opt. Soc. Am. A **23**(10), 2433–9 (2006).
- >> G.L. Charvat. "Low-Cost, High Resolution X-Band Laboratory Radar System for Synthetic Aperture Radar Applications," Austin, Texas: Antennas Measurement Techniques Association conference, October 2006.
- >> T. Gambichler et al. "Characterization of benign and malignant melanocytic skin lesions using optical coherence tomography *in vivo*," J. Am. Acad. Dermatol. **57**(4), 629-37 (2007).
- >> T.S. Ralston et al. "Interferometric synthetic aperture microscopy," Nat. Physics **3**(2), 129–34 (2007).
- >> T.S. Ralston et al. "Real-time interferometric synthetic aperture microscopy," Opt. Express **16**(4), 2555–69 (2008).